JAST, Vol. 4, No. 1, pp 33–38

JAST
Journal of Aerospace Science and Technology

Investigation of Preload Effects on Noncircular Gas Bearing Systems Performance

A. D. Rahmatabadi[1], R. Rashidi[2]

This paper presents the effect of preload on static and dynamic performance characteristics of several gas-lubricated noncircular journal bearing configurations. The linearized system approach using finite element method is used to obtain both steady state and dynamic characteristics.

The results of the investigation show that preload has a significant effect on frictional power loss and the stability margin. It is observed that increased preload lowers the stability margin while will increases the amount of power loss in noncircular gas lubricated bearing systems. The results also show that the preload effect on stability margin is more pronounced at lower compressibility numbers.

NOMENCLATURE

$\overline{B}_{mn}$	$B_{mn}\overline{P}_a\overline{R}^2/\left(\overline{C}_m\overline{w}\right)$, gas film damping coefficients (Ns/m); m,n=x,y
$\overline{C}$	Conventional radial clearance(m), Figure 2.
$\overline{C}_m$	Minor clearance when journal and bearing geometric centers are coincident (m)
$\overline{F}$	$F\overline{P}_a\overline{R}^2$, film force on the journal (N)
$\overline{h}$	$h\overline{C}_m$, film thickness (m)
$\overline{M}_c$	$\overline{M}_c\overline{P}_a\overline{R}^2\left(\overline{C}_m\overline{w}\right)$, critical mass parameter, (kg)
θ	Angular coordinate measured from x-axis, Figure 2
P	$\overline{P}/\overline{P}_a$, subambient gas pressure
$\overline{P}_a$	Ambient pressure(N/m^2)
$\overline{P}_L$	$P_L\overline{\mu}\overline{R}^4\overline{\omega}^2/\overline{C}_m$, frictional power loss (Watt)
$\overline{S}_{mn}$	$S_{mn}\overline{P}_a\overline{R}^2/\overline{C}_m$, gas film stiffness coefficients (N/m); m,n=x,y
F_0	Bearing load capacity
x, y	Cartesian axes with origin at bearing geometric center, subscript for components
δ	$\overline{C}_m/\overline{C}$ preload the bearing
ϕ	attitude angle
γ	Whirl frequency ratio at the threshold of instability
λ	Bearing length to diameter ratio, aspect ratio
Λ	$6\overline{\mu}\overline{\omega}\overline{R}/\left(\overline{P}_a\overline{C}_m^2\right)$ compressibility number
$\overline{\mu}$	Ambient dynamic viscosity of the lubricant (Ns/m^2)
$\overline{\omega}$	Rotational speed of the journal (1/s)
ξ	$\overline{\xi}/\overline{R}$,coordinate along bearing axis measured from midspan
0	Subscript for steady state

INTRODUCTION

During the past few decades gas lubricated bearings have received great attention of practicing and analytical tribologists. The rapid growth of gas bearing technology is mainly due to their wide ranging engineering application. Gas bearings are now used in turbines, aerospace inertial guidance system, precision machine tools, nuclear power equipment, *etc.* In all these applications gas bearings are preferred because of some of their unique features, such as no contamina-

1. *Assisstant Professor, Dept. of Mech. Eng., Yazd Univ., Yazd, Iran, Email: dashti@yazduni.ac.ir.*
2. *M.Sc. Student, Dept. of Mech. Eng., Yazd Univ., Yazd, Iran.*

tion, stability of lubricant over wide temperature range, abundant supply of air as lubricant, less frictional power losses and several others.

The advantages of gas bearings are, however, debased by two familiar shortcomings, namely the low load capacity and the poor dynamic stability due to self excited whirl. Fortunately, the gas bearings in practical applications are subjected to light loads. The problem of dynamic instability is more severe in gas bearings than that in oil bearings due to higher speed of gas bearing applications and low viscosity of the lubricant, *i.e.* gas. To overcome the instability problem lobed gas bearings have been suggested in which the amount of preload (δ) of a lobed bearing determines its noncircularity or ellipticity relative to a plane journal bearing. For zero preload, the journal touches the lobes at their line of centers while with unit preload a lobed bearing reduces into an axial groove plane journal bearing [1].

In the literature on both oil and gas lubricated lobed bearings the preload has usually been taken as 0.5.

The present work investigates the effect of preload on performance of two-lobe, three-lobe and four-lobe bearings (Figure 1).

The dynamic analysis is based on Lund's work [2,3] and the author's previous works on stability problem of linearized gas lubricated plane journal bearing systems [4-7]. Nevertheless, Chandra *et.al.* [8] studied four gas lubricated noncircular journal bearing configurations at $\delta = 0.5$ only. The goal of this paper is to obtain the effect of different preload values on static and dynamic performance characteristics of noncircular gas bearing systems. The analysis describing the governing equations and their solution is given in the next section.

ANALYSIS

The geometric details of a noncircular bearing configuration are shown in Figure 2.

Analysis of gas lubricated noncircular bearing involves solution of the governing equations separately for an individual lobe of the bearing, treating each lobe as an independent partial bearing. To generalize the analysis for all noncircular geometries, the film

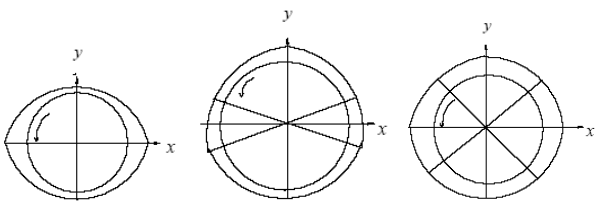

Figure 1. Noncircular journal bearing configurations, (a) Two lobe, (b) Three lobe, (c) Four lobe.

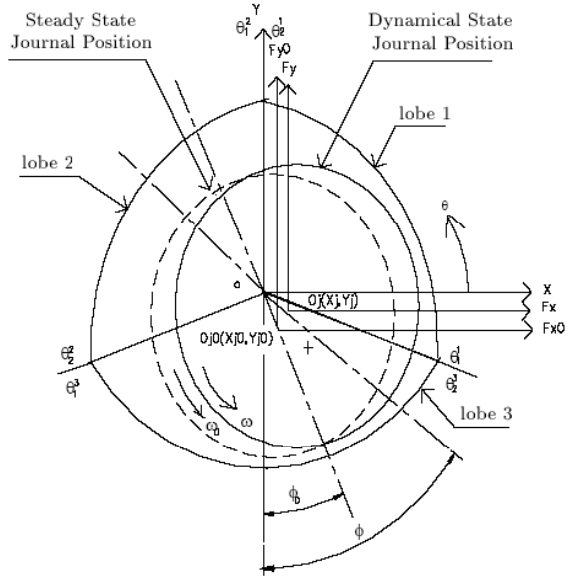

Figure 2. Noncircular (three-lobe) bearing geometry and coordinate axes.

geometry of each lobe is described with reference to bearing fixed cartesian axes (Figure 2). Thus, the film thickness in the clearance space of the Kth lobe, with the journal in a state of translatory whirl, is expressed as [8]:

$$h_k = \frac{1}{\delta} - X_j \cos\theta - Y_j \sin\theta + (\frac{1}{\delta} - 1)\cos(\theta - \theta_0^k), \quad (1)$$

and

$$h_{ok} = \frac{1}{\delta} - X_{j0} \cos\theta - Y_{j0} \sin\theta + (\frac{1}{\delta} - 1)\cos(\theta - \theta_0^k), \quad (2)$$

is the steady state film thickness. (X_{j0}, Y_{j0}) and (X_j, Y_j) are respectively the steady state and dynamic journal center coordinates and θ_0^k is angle of lobe line of centers. The pressure governing equation of isothermal flow field in a bearing lobe is [9]:

$$\frac{\partial}{\partial\theta}\left\{h^3(P+1)\frac{\partial P}{\partial\theta}\right\} + \frac{\partial}{\partial\xi}\left\{h^3(P+1)\frac{\partial P}{\partial\xi}\right\} = \Lambda\left[U\frac{\partial}{\partial\theta} + 2\frac{\partial}{\partial t}\right]\{(P+1)h\}, \quad (3)$$

subjected to the conditions:

$$P(\theta_1^k, \xi, t) = P(\theta_2^k, \xi, t) = P(\theta, \pm\lambda, t) = 0, \quad (4)$$

where θ_1^k and θ_2^k are respectively, the leading and trailing edge boundaries of Kth lobe. To describe the dynamic state of the flow field, the whirling motion of the journal is assumed to be harmonic [2,3], that is:

$$\begin{cases} X' = \mathrm{Re}\left(|X'|\, e^{j\gamma t}\right) \\ Y' = \mathrm{Re}\left(|Y'|\, e^{j\gamma t}\right) \end{cases} \quad (5)$$

where X',Y' are the perturbation coordinates of the journal measured from its static equilibrium position and $|X'|$,$|Y'|$ are the motion amplitudes and $j = \sqrt{-1}$.

The gas pressure may be expressed as the sum of the steady state pressure (P_0) and the dynamic pressure. Thus, to a first approximation:

$$P = P_0 + P'_x X' + P'_y Y', \tag{6}$$

where:

$$P'_x = P_x + j\gamma P_{\dot{x}}, \quad P'_y = P_y + j\gamma P_{\dot{y}}, \tag{7}$$

are the dynamic pressure components. The steady state pressure equation, obtained by substituting Eq.(6) in Eq.(3) and putting $X' = Y' = 0$, is:

$$\frac{\partial}{\partial\theta}\left\{h_0^3\,(P_0+1)\,\frac{\partial P_0}{\partial\theta}\right\} + \frac{\partial}{\partial\xi}\left\{h_0^3\,(P_0+1)\,\frac{\partial P_0}{\partial\xi}\right\} = \Lambda\frac{\partial}{\partial\theta}\left[(P_0+1)\,h_0\right]. \tag{8}$$

The equations for P'_x and P'_y are obtained by partial differentiation of Eq. (3) with respect to X' and Y'. Thus:

$$\begin{aligned}
&\frac{\partial}{\partial\theta}\left\{h_0^3(P_0+1)\frac{\partial P'_z}{\partial\theta} + h_0^3\frac{\partial P_0}{\partial\theta} - \Lambda h_0 P'_z\right\} \\
&+ \frac{\partial}{\partial\xi}\left\{h_0^3(P_0+1)\frac{\partial P'_z}{\partial\xi} + h_0^3\frac{\partial P_0}{\partial\xi}P'_Z\right\} - j2\gamma\Lambda h_0 P'_z \\
&= \frac{\partial}{\partial\theta}\left\{f(\theta)(P_0+1)\left(3h_0^2\frac{\partial P_0}{\partial\theta} - \Lambda\right)\right\} \\
&+ \frac{\partial}{\partial\xi}\left\{3h_0^2 f(\theta)(P_0+1)\frac{\partial P_0}{\partial\xi}\right\} - j2\gamma\Lambda(P_0+1)f(\theta),
\end{aligned} \tag{9}$$

where P'_z stands for P'_x or P'_y, that is:

$$P'_z = P_z + j\gamma P_{\dot{z}}, \quad z = x, y \tag{10}$$

and

$$f(\theta) = \begin{cases} \cos\theta & \text{for } P'_x \\ \sin\theta & \text{for } P'_y \end{cases} \tag{11}$$

In this work, the solution of Eq. (8), which is nonlinear, has been obtained by Newton's method using a finite element technique as did Rohde and Oh [10]. The equations can easily be framed using Galerkin's method [11]. The resulting finite element equations would however be complex. Some details of the respective boundary conditions and solutions are given here.

The global finite element equations (Eq. (9)) may be written in the form:

$$[F_z]\{P'_z\} + \{Q_z\} = \{H_z\}. \qquad (z = x, y) \tag{12}$$

These equations represent a set of complex linear simultaneous equations in nodal pressures ($\{P'_z\}$) and flows ($\{Q_z\}$) and may be solved after incorporating the boundary conditions at the nodes. The nodal conditions are that P'_z equals zero at the boundary nodes (Eq. (4)) and that Q_z is zero at all internal nodes. Thus, to apply the nodal conditions all column elements of the [F] matrix, except the diagonal element, corresponding to a boundary node are set to zero. The diagonal element is set equal to unity. Eq. (12) is now reframed as:

$$\begin{bmatrix} [F_z^r] & -[F_z^i] \\ [F_z^i] & -[F_z^r] \end{bmatrix} \begin{Bmatrix} \{P_z\} \\ \{\gamma P_{\dot{z}}\} \end{Bmatrix} + \begin{Bmatrix} \{Q_z^r\} \\ \{Q_z^i\} \end{Bmatrix} = \begin{Bmatrix} \{H_z^r\} \\ \{H_z^i\} \end{Bmatrix}, \tag{13}$$

where the superscripts 'r' and 'i' represent, respectively, the real and the imaginary parts of the matrices. Eq. (13) may now easily be solved for P_z and $\gamma P_{\dot{z}}$.

STATIC CHARACTERISTICS

Having obtained the steady state pressure field by the solution of Eq. (8), the static characteristics are obtained, which are described by the bearing load capacity, the attitude angle and the viscous power loss. The components of the gas film force on the journal are given by:

$$\begin{bmatrix} F_{x0} \\ F_{y0} \end{bmatrix} = \sum_{k=1}^{L} \begin{bmatrix} F_{x0}^k \\ F_{y0}^k \end{bmatrix} = -\sum_{k=1}^{L} \int_{-\lambda}^{\lambda} \int_{\theta_1^k}^{\theta_2^k} P_{0k} \begin{bmatrix} \cos\theta \\ \sin\theta \end{bmatrix} d\theta d\xi, \tag{14}$$

where L stands for the number of lobes. The load capacity and the attitude angle are then given by:

$$\begin{cases} F_0 = (F_{X0}^2 + F_{Y0}^2)^{\frac{1}{2}} \\ \phi_0 = arctan\,(X_{j0}/Y_{j0}) \end{cases} \tag{15}$$

the viscous power loss is given by [8]:

$$P_L = \sum_{K=1}^{L} \int_{-\lambda}^{\lambda} \int_{\theta_1^k}^{\theta_2^k} \left(\frac{3h_{0k}}{\Lambda}\frac{\partial P_{0k}}{\partial\theta} + \frac{1}{h_{0k}}\right) d\theta d\xi. \tag{16}$$

DYNAMIC CHARACTERISTICS

The components of resultant gas film force on the journal may be expressed as:

$$\begin{aligned}
\begin{Bmatrix} F_x \\ F_y \end{Bmatrix} &= \begin{Bmatrix} F_{x0} \\ F_{y0} \end{Bmatrix} - \begin{bmatrix} Z_{xx} & Z_{xy} \\ Z_{yx} & Z_{yy} \end{bmatrix} \begin{Bmatrix} X' \\ Y' \end{Bmatrix} \\
&= -\sum_{k=1}^{L} \int_{-\lambda}^{\lambda} \int_{\theta_1^k}^{\theta_2^k} P_i \begin{Bmatrix} \cos\theta \\ \sin\theta \end{Bmatrix} d\theta d\xi,
\end{aligned} \tag{17}$$

that

$$Z_{mn} = S_{mn} + j\gamma B_{mn}, \qquad (m, n = x, y) \tag{18}$$

It now follows from Eqs. (6) and (17) that:

$$\begin{bmatrix} Z_{xx} & Z_{xy} \\ Z_{yx} & Z_{yy} \end{bmatrix}^T = \sum_{-\lambda}^{\lambda} \int_{\theta_1^k}^{\theta_2^k} \int \begin{bmatrix} P'_x \\ P'_y \end{bmatrix} \begin{bmatrix} \cos\theta & \sin\theta \end{bmatrix} d\theta d\xi. \tag{19}$$

It is clear from Eqs. (7), (18) and (19) that the coefficients S_{mn} correspond to the film force reaction components of real parts of P'_x and P'_y, *i.e.* P_x and P_y. Similarly the coefficients B_{mn} correspond to the film force components of the imaginary parts of P'_x and P'_y, *i.e.* $\gamma\, P_{\dot{x}}$ and $\gamma\, P_{\dot{y}}$. It should also be noted from Eq. (8) that P'_x and P'_y, and hence the gas film dynamic coefficients, depend on the whirl frequency ratio γ.

STABILITY MARGIN

The stability of motion of journal in free translatory whirl are obtained from Eq. (17) and the Newton second law of motion, as:

$$M\begin{bmatrix} \ddot{X}' \\ \ddot{Y}' \end{bmatrix} + \begin{bmatrix} B_{xx} & B_{xy} \\ B_{yx} & B_{yy} \end{bmatrix} \begin{bmatrix} \dot{X}' \\ \dot{Y}' \end{bmatrix} + \begin{bmatrix} S_{xx} & S_{xy} \\ S_{yx} & S_{yy} \end{bmatrix} \begin{bmatrix} X' \\ Y' \end{bmatrix} = \begin{bmatrix} 0 \\ 0 \end{bmatrix}, \tag{20}$$

where M is the journal mass.

Substituting Eq. (5) in Eq. (20) it can easily be shown that the characteristic equation of the translatory limit cycle is:

$$(-M\gamma^2 + S_{xx} + j\gamma B_{xx})(-M\gamma^2 + S_{yy} + j\gamma B_{yy}) - (S_{xy} + j\gamma B_{xy})(S_{yx} + j\gamma B_{yx}) = 0, \tag{21}$$

which on separating the real and imaginary parts gives:

$$M\gamma^2 = (S_{xx}B_{yy} + S_{yy}B_{xx} - S_{xy}B_{yx} - S_{yx}S_{xy})/(B_{xx} + B_{yy}), \tag{22}$$

$$\gamma^2 = [(S_{xx} - M\gamma^2)(S_{yy} - M\gamma^2) - S_{xy}S_{yx}]/(B_{xx}B_{yy} - B_{xy}B_{yx}). \tag{23}$$

The above equation provides the criteria for determination of γ and the stability margins. Quite obviously there would be a unique combination of the frequency ratio and the dynamic coefficients which satisfy Eqs. (9) and (23) simultaneously.

Corresponding to the value of the frequency ratio of the film induced whirling, the stability margin may be expressed from Eq. (22), as:

$$M_c = (S_{xx}B_{yy} + S_{yy}B_{xx} - S_{xy}B_{yx} - S_{yx}B_{xy})/[(B_{xx} + B_{yy})\gamma^2], \tag{24}$$

where M_c will now be referred to as journal mass parameters.

Thus, the dynamic coefficients, critical mass parameter and the whirl frequency ratio at the threshold of instability are determined by trial [2,3].

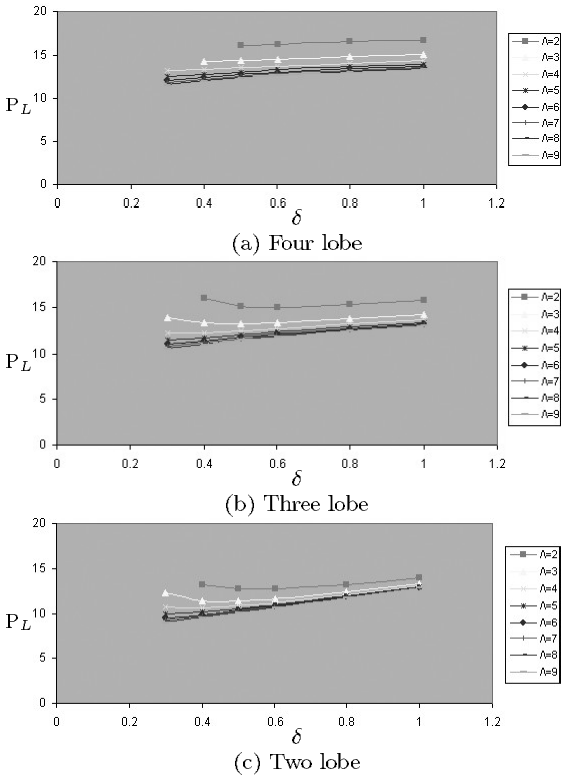

(a) Four lobe

(b) Three lobe

(c) Two lobe

Figure 3. The effect of preload on power loss, P_L.

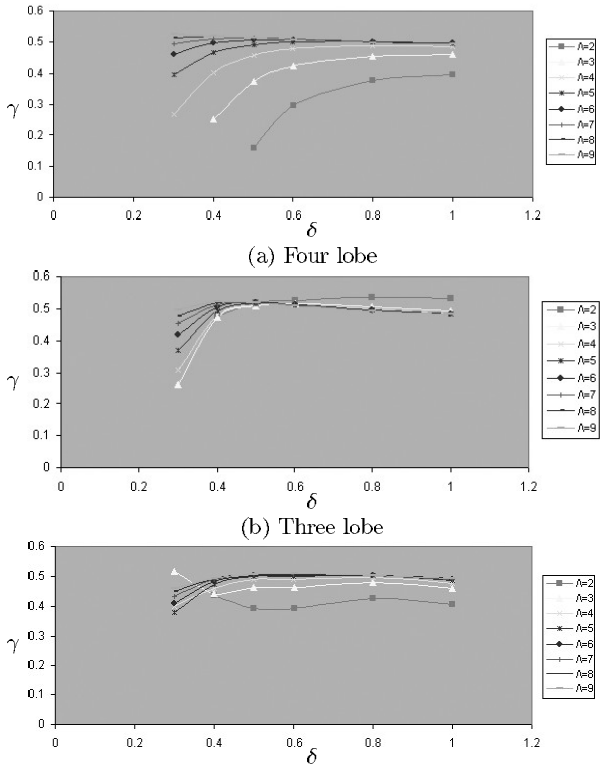

(a) Four lobe

(b) Three lobe

(c) Two lobe

Figure 4. The effect of preload on whirl frequency ratio, γ.

RESULTS AND DISCUSSIONS

In this paper the effect of preload on the three bearing forms, *viz.* two-lobe, three-lobe and four-lobe bearings is investigated. The tilt and mount angles are zero as in Ref. [8] while the bearing load capacity (F_0) has been taken as one. Also the bearing aspect ratio has throughout been taken as unity, which is the most commonly used value in practical applications. Preload variations are taken from 0.3 to 1.0, so that the results also provide a comparison of lobed and axial groove bearings. Table 1 compares our results with those in Ref. [8]. It is seen that the present results are in good match with the reported values in Ref. [8], for $\delta = 0.5$.

The results are:

1. Figure 3 shows the effect of preload value on power loss. It is seen that by increasing the preload factor, *i.e.* by going from a noncircular bearing configuration towards a circular one, the power loss increases. This means that noncircular bearing systems act better than circular bearing for the above aspect. This finding from the point of view of conservation of energy is an important aspect which should be considered while selecting a gas bearing system.
2. The effect of preload on two inter-connected characteristic parameters of bearing system namely whirl frequency ratio and critical mass parameter are depicted in Figures 4 and 5. It is seen that with an increase in the value of preload, the whirl frequency ratios are increased, while at the same time the critical mass ratios acting as the stability parameters are decreased, indicating that noncircular bearing systems are more stable than the circular ones. Keeping in mind that gas bearing systems are already prone to instability due to high operating speeds and low viscosity of lubricant, *i.e.* gas, noncircular bearing systems could be the best selection in such conditions.

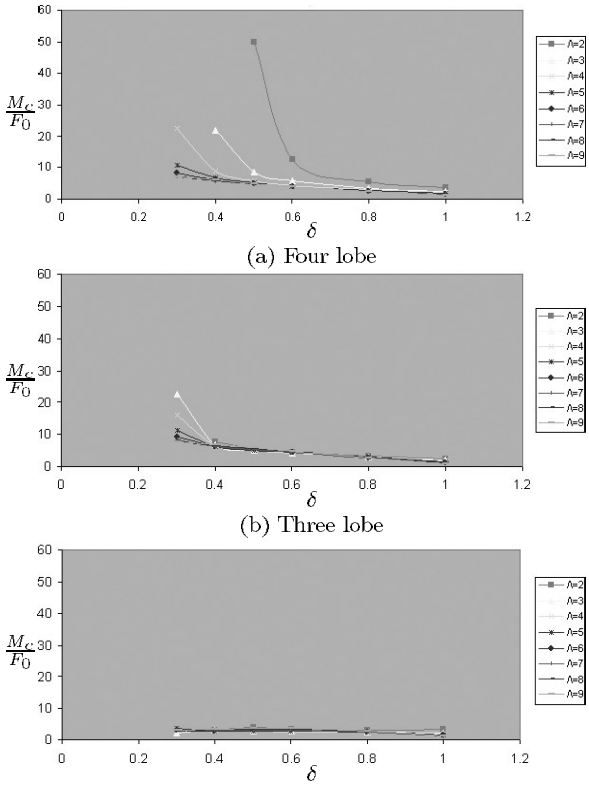

(a) Four lobe

(b) Three lobe

(c) Two lobe

Figure 5. The effect of preload on critical mass, M_c.

3. From Figure 5, it is seen that the lower the compressibility number, the more the effect of preload on critical mass.
4. Results depicted in Figures 3 and 5 also show that among the three noncircular gas bearings chosen for this study, the four lobe bearing system stability parameters are more effected by preload values, while the effect of preload on power loss is almost the same for all the bearing systems considered.
5. Based on the results shown in Figures 3 and 5, it is also seen that we can achieve lower power loss

Table 1. Comparison of static and dynamic characteristics ($\lambda = 1; \delta = 0.5$).

Λ	F_0	Type of bearing	ϕ_0		P_L		γ		M_c	
			*	**	*	**	*	**	*	**
2	0.2	Two-lobe	76.1	76.5	10.22	10.29	0.480	0.488	0.04	0.03
		Three-lobe	68.2	68.6	11.26	11.34	0.418	0.422	0.74	0.72
		Four-lobe	69.1	69.5	11.96	12.00	0.419	0.426	0.63	0.57
5	0.5	Two-lobe	55.8	56.1	10.11	10.16	0.472	0.478	0.29	0.26
		Three-lobe	52.3	52.7	11.22	11.28	0.435	0.437	0.95	0.94
		Four-lobe	54.8	55.4	12.01	12.04	0.508	0.512	1.01	0.98
10	1.00	Two-lobe	34.3	34.9	10.03	10.07	0.460	0.467	0.30	0.29
		Three-lobe	44.2	44.6	11.29	11.31	0.428	0.432	0.76	0.75
		Four-lobe	48.3	48.7	12.26	12.30	0.437	0.441	0.63	0.59

*) Present analysis.

**) Data from Ref[8].

and at the same time higher stability margins at low preload values.

CONCLUSIONS

Based on the results presented above, the following conclusions are drawn:

Preload as a design parameter can be selected to meet some specific design goals. Improvement in the stability characteristics and reduction in frictional power loss of the noncircular bearings can be achieved by selecting the suitable preload values.

High values of preload deteriorate the stability characteristics of the lobed bearings and increase frictional power loss. However, small preloads should also be avoided in lobed bearings as there is a possibility of metal to metal contact in such cases. Considering the above aspect and the results obtained in the investigation it seems that in the preload range $\delta = 0.4 - 0.6$, lobed bearings can have satisfactorily high values of stability parameters as well as optimal frictional power loss.

REFERENCES

1. Feng, F. and Chu, F., "Influence of Preload Coefficient of TPJBs on Shaft Lateral Vibration", *Tribology International*, PP 65-71(2002).
2. Lund, J.W., "A Theoretical Analysis of Whirl Instability and Pneumatic Hammer for a Rigid Rotor in Pressurized Gas Journal Bearings", *J. Lubr. Tech., Trans ASME*, PP 154-166(1967).
3. Lund, J.W., "Calculation of Stiffness and Damping Properties of Gas Bearing", *J. Lubr. Tech., Trans ASME*, PP 793-803(1968).
4. Malik, M., Rahmatabadi, A.D. and Jain, S.C., "An Assessment of The Stability Chart of Linearized Gas-Lubricated Plane Journal Bearing System", *Tribology Transaction*, PP 56-60(1989).
5. Rahmatabadi, A. D., "Dynamic Response of Gas Lubricated Journal Bearing Systems", Ph.D. Thesis, University of Roorkee, Roorkee, India(1992).
6. Rahmatabadi, A.D., Jain, S.C. and Malik,M., "The Transient Response of a Journal in Plane Gas Lubricated Bearing During Acceleration Periods", *Sixth Annual Mechanical Engineering Conference and Third International Mechanical Engineering Conference of the ISME*, PP 69-77(1998).
7. Rahmatabadi, A.D., Malik, M., "Stability of Gas Lubricated Circular Journal Bearing Systems During Acceleration with Aspect Ratio Effects", *Journal of Mechanical Engineering, Transactions of the ISME*, **2**, PP 23-34(2001).
8. Chandra, M., Malik, M. and Sinhasan, R., "Comparative Study of Four Gas-Lubricated Noncircular Journal Bearing Configurations", *Tribology International*, **16**(2), PP 103-108(1983).
9. Frene, J., *Hydrodynamic Lubrication: Bearing and Thrust Bearing*, Costantinescu, Elsevier, (1997).
10. Rohde, S.M. and Oh, K.P., "Higher Order Finite Element Methods for the Solution of Compressibile Porous Bearing Problems", *International Journal for Numerical Methods in Engineering*, PP 903-911(1975).
11. Reddy, J., *An Introduction to the Finite Element Method*, McGraw-Hill, (1984).